

Proceeding of the Korean Nuclear Society Spring Meeting

Cheju, Korea, May 2001

## **The Effects of Non-Condensable Gas on the Critical Pressure Ratio and Critical Flow Rate in a Safety Valve**

Se Won Kim

Korea Institute of Nuclear Safety,

19 Kusung-dong, Yusung-gu, Taejon 305-338, Korea

Hee Cheon NO

Korea Advanced Institute of Science and Technology,

371-1 Ku-song Dong, Yu-song Gu, Taejon 305-701, Korea

### **Abstract**

The effect of non-condensable gas on subcooled water critical flow phenomena in a safety valve is investigated experimentally at various subcoolings and disk lifts. In the experiment, the flow rate of non-condensable gas is controlled between 0 to 2 m<sup>3</sup>/hr about 11 bar after the subcooled water critical condition is established at the throat of a safety valve. The critical pressure ratio with non-condensable gas is increased within 5% variation of that without non-condensable gas while its increase is little affected by non-condensable gas fraction. The subcooled water critical flowrate shows a decreasing trend as the void fraction is increased and its value is about 90% of the subcooled water critical flow rate without non-condensable gas when the gas fraction reaches 40%.

### **1. Introduction**

The depressurization rate of the plant system is limited by critical flow rates through the safety valve. Therefore, the predictions of the flow rates through a safety valve are important for the design of industrial high pressure vessels. Safety valves addressed insofar as saturated steam conditions in the safety analyses and the commercial safety valves were usually designed for steam service. However, the real plant data show that the safety relief valves could be under the situation of water or two-phase conditions. Hence, the U.S. NRC specified that the valves should be tested under the full range of expected operating fluid conditions. The physical phenomenon of two-phase choking flow is not well understood when gas and liquid phases are flowing simultaneously through

a safety valve. In the case of safety valve, the geometrical and subcooling parameters are very influential on the mass flowrate and on the pressure topology. The occurrence of rapid evaporation (flashing) during a discharge of initially subcooled liquid essentially limits the valve capacity. So, the pressure relief system may not operate as it is designed because the safety valve, selected by the means of the traditional sizing methods generally based on the Bernoulli equation, may produce the mass-flow rate too small to adequately reduce the pressure inside an installation. The present knowledge about this phenomenon is insufficient and no theoretical model exists that can adequately predict the two-component critical flow through a safety valve. This research focuses on the visualization of flow patterns, critical pressure ratios, and choked flowrate in a safety valve, including the effect of variable receiver pressures, disk lifts and subcoolings. The developed flow model based on the experimental results accounting for the nonequilibrium effect is compared with other analytical critical flow models of safety valve.

In the short tube geometry, the experimental critical mass flux of the downstream choking approximated the values predicted by both a surface tension model developed by Burnell[1] and a surface evaporation model proposed by Bailey[2]. Burnell hypothesized that the surface tension force retards the formation of vapor bubbles, thereby increases the flow rate. Bailey suggested three definite flow regimes. The first regime is related to considerably subcooled condition at all points and the flow curve is represented by the conventional Bernoulli equation. The second regime is associated with metastable flow condition and the flow curve according to the pressure drop shifts suddenly from the first regime to the second one. The third is related to choking flow condition that resembles gaseous critical flow in its effect. Henry and Fauske[3] developed the non-equilibrium homogeneous two-phase flow critical model, in which the critical flow rate can be obtained from the energy equation frozen at the inlet quality and it is assumed that the vapor formed is saturated at the local pressure.

In the case of a safety valve, the geometrical and subcooling parameters are very influential on the mass flow-rate and on the pressure topology. The thermodynamic non-equilibrium status affected by the geometry is not clear. As the critical condition in a valve strongly depends on the non-equilibrium factors, the observed phenomenon becomes complicated. Several studies have been conducted to clarify the subcooled critical flow in a safety valve and a control valve [4,5,6,7]. Their experiments focus on the flow rate and the discharge coefficient of valve. They do not observe the pressure characteristics between the disk and seat surface area (throat or curtain area) because it is not easy to get the data of pressure behavior at the real throat position of the valve.

It can be summarized that there is not only a lack of knowledge regarding the mechanism involved in the flashing of compressed water through a safety valve, but some uncertainty regarding the flow characteristics in a safety valve at such flow situations. Therefore, this research focuses on the detection of critical pressure ratio and the calculation of choked flow rate in a safety valve, including the effect of void fraction, receiver pressures, disk lifts and subcoolings. With these informations it might be possible to more thoroughly understand the critical characteristics of metastability in rapid expansion of two phase mixture in a safety valve.

## 2. Safety Valve Critical Flow Model

Under the normal condition of flow, the flow rate is proportional to the pressure drop through a valve. However, vapor cavities form when the vena contracta pressure drops below the saturation pressure of liquid with the increase in pressure drop across the valve. Proportionality deteriorates with the vapor formation and flow becomes completely choked when sufficient vapor has formed, so that there may be no increase in flow rate as the valve pressure drop increases. In case of a safety valve, the disk exit pressure is considered to be the throat (vena contracta) pressure and it is the dominant parameter to calculate the flow rate.

Generally, the throat pressure is the unknown variable in a safety valve. Therefore, the valve outlet pressure is used to calculate the flow rate of safety valve. In a safety valve, the flow rate is determined by the Bernoulli equation when the pressures of the inlet and outlet regions are at sufficiently high and the fluid is considerably subcooled in both regions:

$$G_{cr.Pout} = K_d \sqrt{2 \mathbf{r}_f (P_{in} - P_{out})} \quad \text{for } L/D=0, \quad (1)$$

where  $K_d$  is the valve discharge coefficient (0.61 is recommended for the case of orifice), and  $\mathbf{r}_f$ ,  $P_{in}$  and  $P_{out}$  denote the density of inlet fluid, the inlet pressure and the outlet pressure, respectively. The flowrate calculation of a safety valve is severely affected by the valve coefficient that is given by the valve vender. In a safety valve, the valve coefficient is strongly affected by the disk lifts and by the subcoolings whose effects have not been analyzed systematically.

Fauske[8] performed various experiments on a 0.25 inch inner diameter channels with a sharp edged entrance and the length-to-diameter,  $L/D$ , ratios between 0(an orifice) and 40. The critical pressure ratio was found to be 0.55 for the long channels in which the  $L/D$  ratio exceeds 12. For  $L/D$  values greater than zero, but less than 12, he recommends to use the following Eqn.:

$$G_{cr.Pcr} = K_d \sqrt{2 \mathbf{r}_f (P_{in} - P_{cr})} \text{ for } L/D > 0, \quad (2)$$

where  $P_{cr}$  is the throat critical pressure determined by experimental data. If the throat pressure is known, the critical flowrate can be estimated more exactly.

In a safety valve, the mass flux of initially compressed water is determined from the Eqn. (1) and a dimensionless mass flux is obtained by dividing this equation by  $(\mathbf{r}_{in} \cdot P_{in})^{1/2}$ , which gives:

$$\hat{G}_{out} = K_d \sqrt{2(1 - P_{out}/P_{in})} \quad (3)$$

In the real system, the flow is subjected to restriction by the throat pressure thus the dimensionless mass flux is expressed in terms of the throat pressure,  $P_t$ , as follows:

$$\hat{G}_t = K_d \sqrt{2(1 - P_t/P_{in})} \quad (4)$$

If we know the critical pressure and the density of the two-component mixture, the critical flow can be calculated by the above four equations. However, there are three unknowns: the critical pressure, the density of the two-component mixture, and the valve discharge coefficient. These values can be determined from experimental data .

### 3. Experimental Apparatus and Procedure

The experimental main apparatus consists of a steam generator, a collection tank, nitrogen gas delivery system, and test section. A schematic of the experimental facility and test section is shown in Fig. 1. These main equipments are connected by 2.5 cm valves and piping. The capacity of the steam generator is 1.3 cubic meters and a 100 kW electric heater is submerged in the tank bottom region. In the test section, the visual windows are installed for the visualization of the flow and void patterns at the inlet and outlet of the valve disk. The disk position of the safety valve can be fixed to any desired lift from 0 to 6 mm using the top mounted micrometer on the test section.

The water temperature in the tank is controlled automatically using the preset temperature switch. The tank pressure is maintained to be constant during the experiment by means of

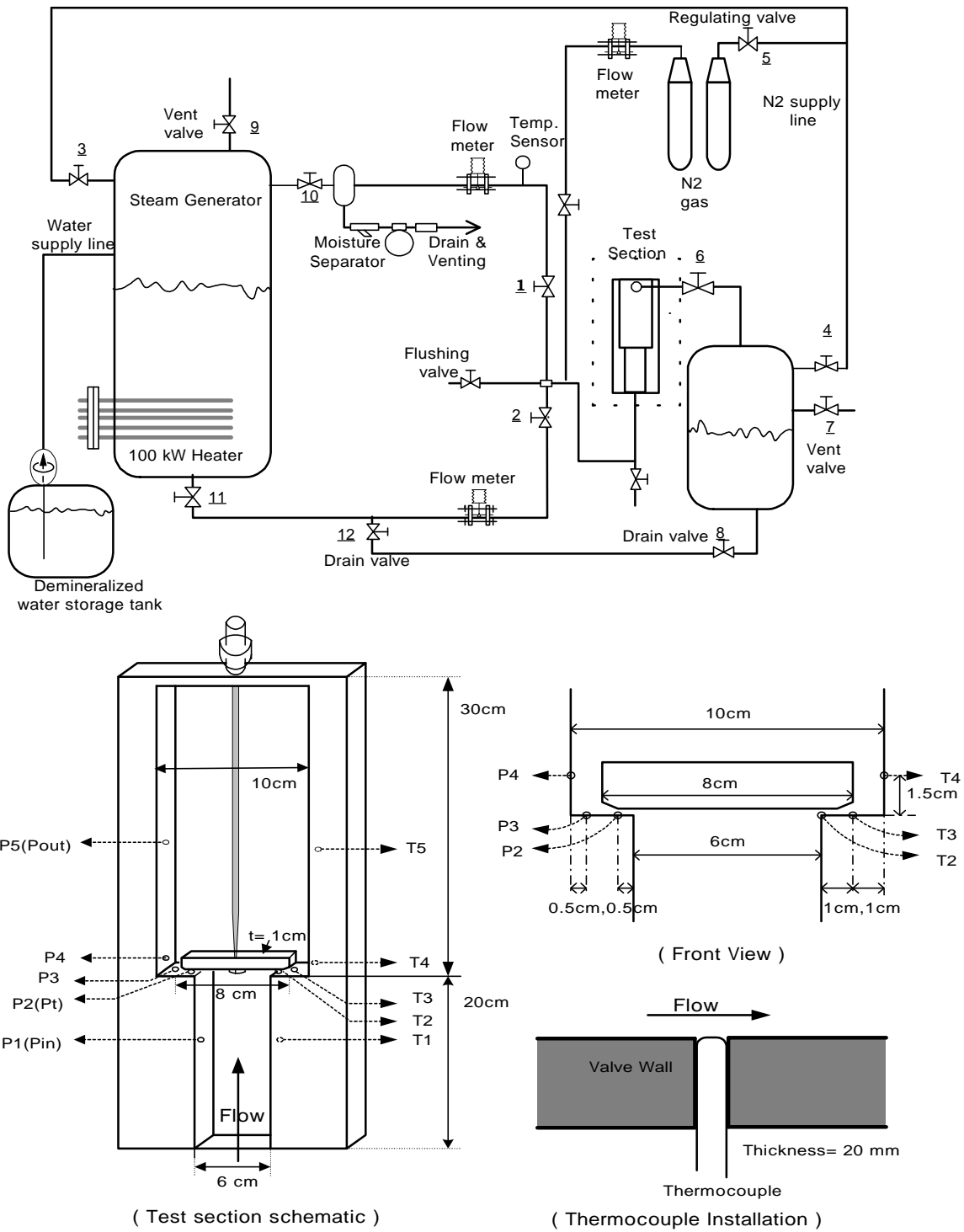


Fig. 1 Schematic drawing of experimental facility and test section

compressed nitrogen and regulating valve. The test line is preheated using the heated water originating from the steam generator.

The hot water flow rate is measured by the hot-water-flow-transmitter that is installed in the horizontal pipe between the steam generator and the test section. The nitrogen gas flow rate is measured by the gas-flow-transmitter that is installed in the horizontal pipe between the nitrogen gas supply system and the test section. The temperatures of the test section are obtained from 5 temperature transmitters, and the temperatures of the steam generator and the collection tank are also monitored by temperature gages. Seven pressure transmitters are used to get the pressure trends during transient and choking condition. Five pressure transmitters are connected to the test section and two pressure transmitters are connected to the inlet and outlet pipes of the test section. The hole diameter of the pressure and thermocouple taps in the test section is selected as 2mm to minimize the effect of nucleation in the disk area.

The instrument accuracies of hot water flowmeter, nitrogen gas flowmeter, pressure transmitter, and temperature transmitter are  $\pm 1\%$ ,  $\pm 1\%$ ,  $\pm 0.1\%$ , and  $\pm 0.1\%$ , respectively. The output signal of each variable ranges from 4 to 20 mA. Hence, using the converter with the accuracy of 0.2%, they are changed from 1 to 5 Volts and recorded to the personnel computer every 1 sec. The data acquisition system has the 12 bit resolution for the 5 Volts and the equivalent error is 0.01 Volt. The uncertainties of instrumentation are summarized at the Table 1.

Table 1. Data acquisition system and uncertainty of instrumentation

Variable	Range	Accuracy	Type	Computer Input Signal	Converter Error	Total Error
Hot Water Flow	0 - 6000 l/hr (0 - 6 m <sup>3</sup> /hr)	1 %	Vortex	1-5 Volt	0.2%	1.02%
Nitrogen Gas Flow	0 - 2000 l/hr (0 - 2 m <sup>3</sup> /hr)	1 %	Thermal Mass	1-5 Volt	0.2%	1.02%
Pressure	0 - 20 bar	0.1 %	Diff. Pres	1-5 Volt	0.2%	0.23%
Temperature	0 - 200	0.1 %	K-Type	1-5 Volt	0.2%	0.23%

To analyze the effects of void fraction and subcooling on the critical flow parametrically, the disc inlet pressures are maintained close to 1 MPa(g), subcoolings are between 10 K and 150 K, and the gas injection is controlled between 0 and 2 m<sup>3</sup>/hr. Table 2 shows the test matrix of present experiment.

Table 2. Test matrix of present experiment

Test Number	Disk Lift(mm)	$P_{in}$ (MPa)	$T_{in}$ (°C / K)	$T_{sub}$ (K)
HW01	1	0.975	55 / 328.15	123.97
HW02	1	1.01	127 / 400.15	53.32
HW03	1	1.025	141.8 / 414.95	39.16
HW04	1	1.0	161 / 434.15	19
HW05	2	0.95	62 / 335.15	115.67
HW06	2	0.94	125 / 398.15	52.21
HW07	2	0.98	145 / 418.15	34.01
HW08	2	1.0	164 / 437.15	16
HW09	3	0.75	57.5 / 330.65	110.26
HW10	3	0.85	124.5 / 397.65	48.44
HW11	3	0.85	145 / 418.15	27.94
HW12	3	0.875	161 / 434.15	13.16
TP01	1.6	9	25 / 298.15	150.54
TP02	1.6	8.5	25 / 298.15	147.94
TP03	1.6	8.85	65 / 338.15	109.64
TP04	1.6	9	75 / 348.15	100.36
TP05	1.6	9	125 / 398.15	50.36
TP06	1.6	9	131 / 404.15	44.36
TP07	1.6	9.75	150 / 423.15	28.97

## 4. Experimental Results and Discussion

### 4-1 General phenomena at the critical state

One-component critical flow features are characterized by constant maximum flow and constant throat pressure when the pressure difference between inlet and outlet of a safety valve is

large enough and still shows increasing trends. This phenomenon also occurs in the two-component flow. Figure 2 and 3 show two typical experimental results of one and two component tests.

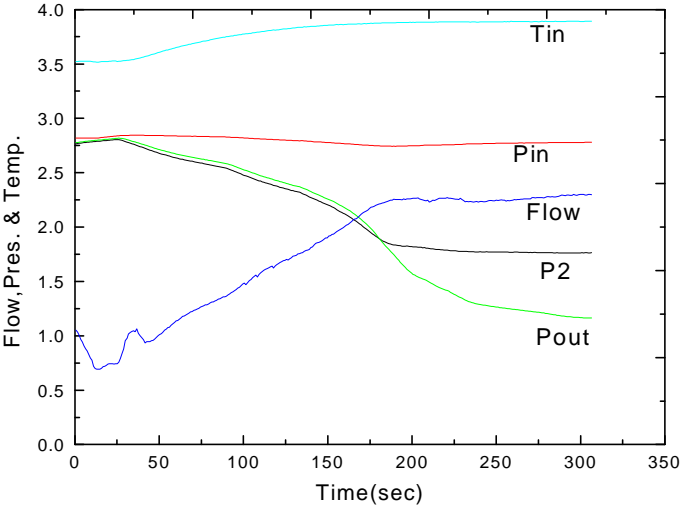


Fig.2 Typical experimental result of subcooling water

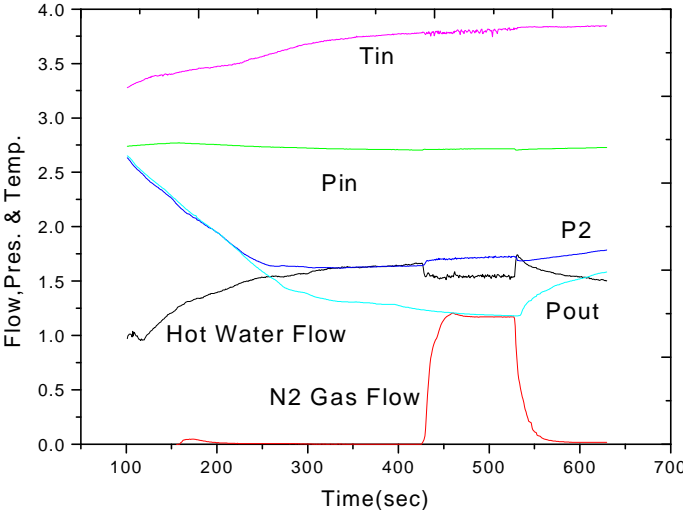


Fig.3 Typical experimental result of subcooling water with the injection of nitrogen gas

From Fig. 2, it can be seen that the outlet pressure(Pout) becomes smaller than the throat



pressure ( $P_2$ ) and constant choking flow characteristics come out distinctly. In the low subcooling water tests, flashing starts at the disk exit and the downstream region of the disk is occupied by steam, when the pressure difference between the inlet and the exit of the disk is large enough. In the high subcooling water tests, some voids generated just downstream of the disk are seen, even though water at the exit of the disk is still subcooled. The voids collapsed soon in the downstream region and this region is filled with cold water. It is presumed that cavitation may take place due to the strong local circulation flow generated at the disk exit. This may explain why highly subcooled water in the valve tests is choked at a velocity much lower than the liquid-only sonic velocity[9]. In the case of nitrogen injection test, the subcooled water critical condition is assured by the constant flow rate and then nitrogen gas is injected into the pipe before the test section. Gas injection pressure is 11 bar and its flowrate is controlled between 130 and 1800 m<sup>3</sup>/hr. Figure 3 shows typical experimental result of subcooling water with the injection of nitrogen gas. Due to the gas injection, the subcooled water critical flowrate decreases sharply and its value is decreased about 7% compared with the subcooled water only critical flow rate. The critical pressure ratio is also affected by the gas injection. Before gas injection, the critical pressure ratio is 0.44 and it increases 0.48 after gas injection.. As the critical state can be evaluated by the constant throat pressure and constant flow, the critical pressure ratio and the critical flow characteristics are reviewed in this section considering the subcooling, disk lift, and the pressure ratio of outlet to inlet of the disk for the subcooling water. Finally, non-condensable gas inclusion effects are also evaluated.

#### 4-2 Critical pressure ratio

The throat critical pressures come out vividly from high subcooling waters to low subcooling waters as decreasing the back pressure of the test section. The measured critical pressure ratios ( $P_{cr}/P_{in}$ ) can be defined by a function of valve inlet pressure, inlet temperature, pressure difference of valve in and out, and disk seat length and lift. The non-dimensional expression of these parameters is defined as follows:

$$\begin{aligned}
 P^* &= P_{out}/P_{in}, \\
 T^* &= T_{sub}/T_{in}, \\
 L^* &= \text{Disk Lift} / \text{Seat Length},
 \end{aligned}
 \tag{5}$$

where  $P_{out}$  is disk outlet pressure(0.1 - 0.3 MPa),  $P_{in}$  is disk inlet pressure(0.85 - 1 MPa),  $T_{in}$  is valve disk inlet water temperature(323.15 - 438.15 K), and  $T_{sub}$  is saturation temperature of  $P_{in}$

minus  $T_{in}$  (10 - 150 K). The ranges of  $P^*$ ,  $T^*$ , and  $L^*$  are 0.10-0.33, 0.03-0.38, and 0.2-0.6, respectively. During the test, the constant throat pressure characteristic exists when the downstream pressure decreases sufficiently. This throat pressure is called the critical pressure ( $P_{cr}$ ). The experimental results of critical pressure ratios are shown in Table 3. These pressure ratios of

Table 3. critical pressure ratio for the different subcoolings and disk lifts

Tsub(K)	Lift,1.6mm After N2	Lift,1.6mm Before N2	Lift,1mm	Lift,2mm	Lift,3mm
123.97			0.24		
53.32			0.42		
38.32			0.49		
19.88			0.64		
115.67				0.28	
52.21				0.42	
34.01				0.49	
15.88				0.58	
109.76					0.26
52.94					0.275
27.94					0.42
12.16					0.56
150.36	0.376	0.332			
147.94	0.373	0.33			
109.64	0.315	0.292			
50.36	0.416	0.398			
49.88	0.408	0.376			
43.69	0.425	0.4			
31.97	0.48	0.44			

high subcooled water ( $T^*=0.38$ ) and low subcooled water ( $T^*=0.03$ ) are about 0.25 and 0.6, respectively. They increase as the subcoolings or disk lifts decrease. One interesting result of  $P_{cr}/P_{in}$  in the low subcooled water ( $T^*=0.03$ ) test is almost the same as the theoretical critical pressure

ratio of wet saturated steam of 0.58 [10]. Using the experimental results and SAS computer program, the correlation of the critical pressure ratio is developed as follows:

$$P_{cr}/P_{in} = 0.15066(P^*)^{0.01542} (T^*)^{-0.3604} (L^*)^{-0.191} \tag{6}$$

Equation (9) shows that the critical pressure ratio is highly affected by  $T^*$ , while the effect of  $P^*$  and  $L^*$  on the critical pressure ratio is relatively small. Figure 8 shows the comparison between measured and predicted critical pressure ratios.

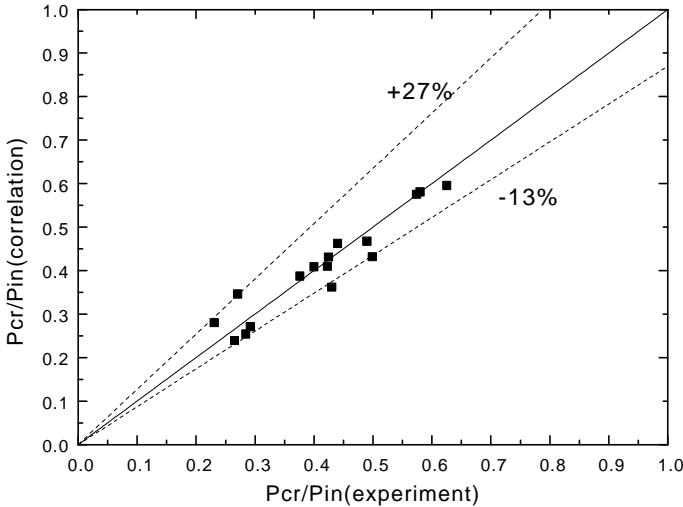


Fig. 4 Comparison between measured and predicted critical pressure ratio

There is good agreement between the measured data and the developed correlation with the deviation of +27% and -13%.

**4-3 Dimensionless mass flux and valve coefficient**

Figure 6 shows two typical high and low subcooling flow trends according to the pressure ratio of  $P_{out}/P_{in}$ . From Fig. 6, it is evident that the measured flow rate is well represented by Eqn. (4) and the determined valve coefficients,  $Kd$ , are 0.73 and 0.76 for the test number HW06 and HW08, respectively. However, there is a wide discrepancy between the measured flow rate and Eqn. (3). Therefore, for the prediction of the flow rate through a safety valve it is better to use the parameter,  $P_t/P_{in}$  instead of  $P_{out}/P_{in}$ .

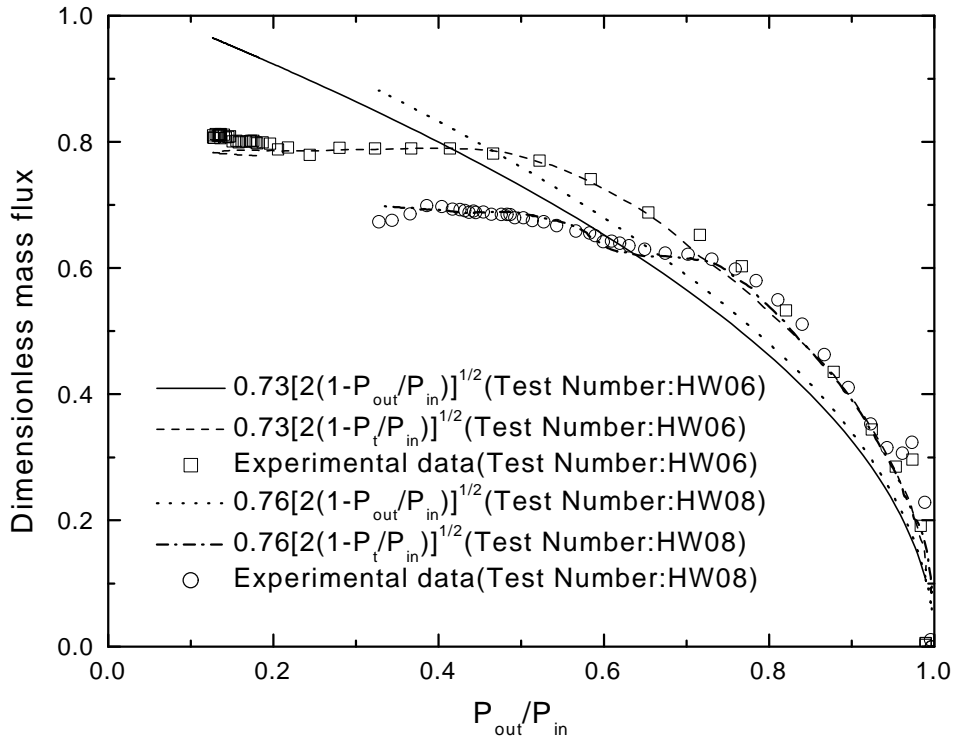


Fig.5 Experimental and calculated dimensionless flowrate as a function of inlet to outlet pressure ratio(HW06 and HW08)

In a safety valve, the critical mass flux of initially compressed water is determined from the Eqn. (2) and dimensionless mass flux is obtained by dividing this equation by  $(r_{in} \cdot P_{in})^{1/2}$ , which gives:

$$\hat{G}_{cr} = K_d \sqrt{2(1 - P_{cr}/P_{in})}. \quad (6)$$

From Eqns. (4) and (6), the critical flow correlation can be written as:

$$\hat{G}_{cr,corr} = K_d \sqrt{2(1 - 0.15066(P^*)^{0.01542} (T^*)^{-0.3604} (L^*)^{-0.191})} \quad (7)$$

Since the valve coefficient is defined as measured flowrate to theoretical flowrate, it can be acquired using the experimental result and Eqn. (7).

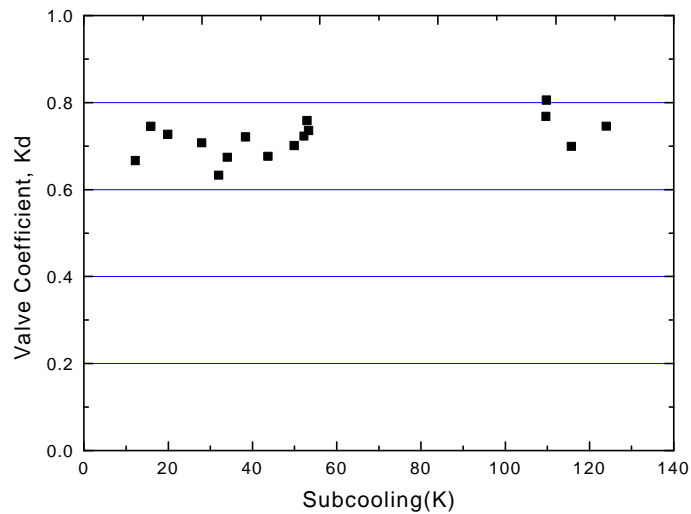


Fig.7 Valve coefficient according to the subcooling

Figure 7 shows the valve coefficient according to the subcooling. As explained above, if we could find the throat pressure, the flow rate is calculated exactly regardless of choking condition accomplished or not. During the choking condition of subcooled water, the valve coefficients are ranged between 0.6 and 0.8 and there is no difference for the change of subcooling.

#### 4-4 Non-condensable Gas Effects on the Critical Mass Flux

The expected mass flow rate is increased with the increase in the inlet subcooling while its effects on the outlet to inlet pressure ratio and disk lift are not clear. When a non-condensable gas is included in a subcooled flow regime, the estimation of two-component flowrate is almost impossible. Therefore, this section briefly compares the one and two-component test results concerning to the critical pressure ratio and critical mass flux. Figure 8 shows the non-condensable gas effect on the critical pressure ratio. The critical pressure ratio shows an increasing trend with the decreasing of subcooling. Figure 8 clearly shows a non-condensable gas inclusion effect and the critical pressure ratio increases slightly. Figure 9 shows the non-condensable gas effect on the critical mass flux. The critical mass flux generally shows a decreasing trend with the decreasing of subcooling. Figure 9 clearly shows a non-condensable gas effect and the critical mass flux decreases slightly. Figure 10 displays the gas fraction effect on the critical pressure ratio and critical flow rate.

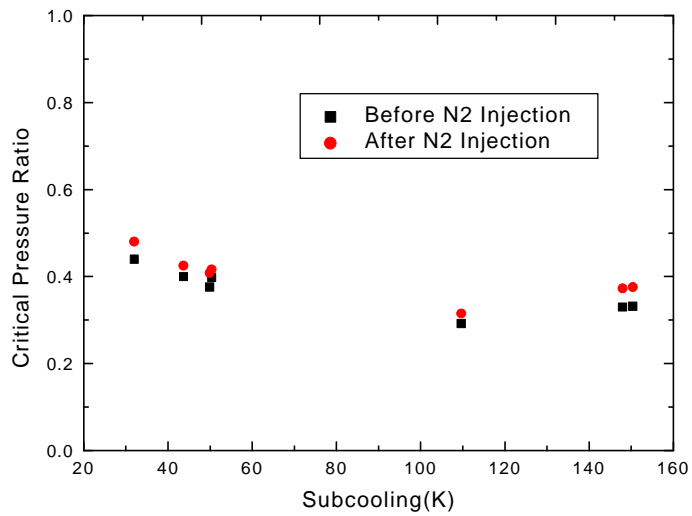


Fig. 8 Nitrogen gas injection effect on the critical pressure ratio

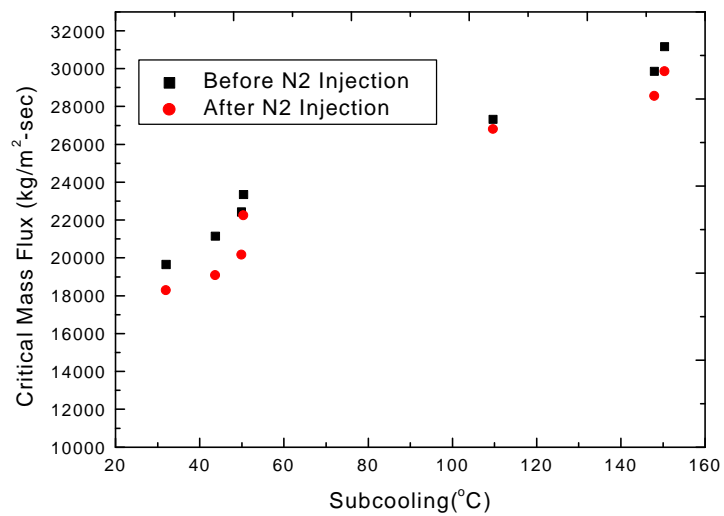


Fig. 9 Nitrogen gas injection effect on the critical mass flux

The critical pressure ratio shows little differences with a variation of the void fraction increasing while critical mass flux shows a decreasing trend with the increasing of void fraction. Due to the injection of nitrogen, the critical pressure ratio increases between 2 and 5% and critical mass flux

decreases about 10% when the void fraction reaches 40%.

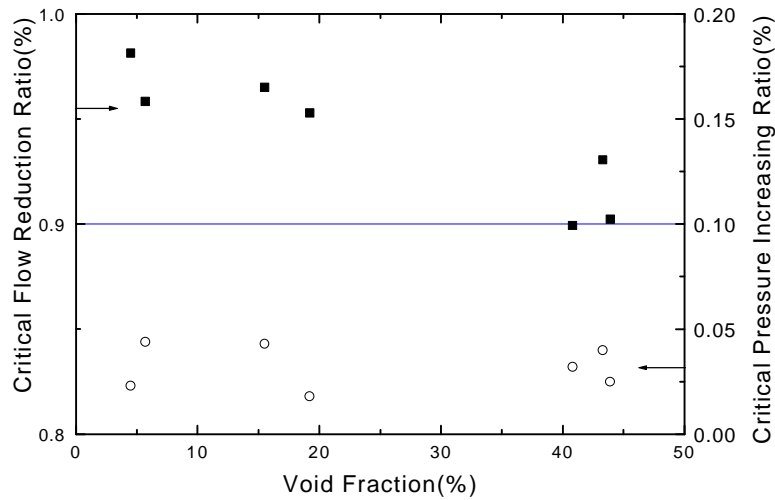


Fig 1 Gas fraction effect on the critical pressure ratio and critical flow rate.

## 5. Conclusions

This study is to provide new experimental results for the critical flow characteristics of non-condensable gas in subcooling water flow in a safety valve. The general critical characteristics of subcooled water for the inclusion of nitrogen gas and different disk lifts are summarized as follows:

- (1) The subcooling water critical flow rate through the safety valve is mainly governed by inlet subcooling while the effect of disk lift and inlet pressure on the critical flow rate is relatively small.
- (2) During the chocking condition of subcooling water, the valve coefficients are ranged between 0.6 and 0.8 and there is no differences for the change of subcooling.
- (3) The critical pressure ratio shows increasing trend with the decreasing of subcooling and it is increased slightly with the inclusion of non-condensable gas.
- (4) Due to the inclusion of non-condensable gas on the upstream flow region, the critical pressure ratio increases between 2 and 5% and critical mass flux decreases about 10% when the gas fraction reaches 40%.

## References

- [1] J.G. Burnell, "Flow of Boiling Water Through Nozzles, Orifices and Pipes," *Engineering*, Vol.164, (1947) 572-576.
- [2] J.F.Bailey, "Metastable Flow of Saturated Water," *Trans. ASME*, Vol.73, (1951) 1109-1116.
- [3] R.E.Henry and H.K.Fauske, "The Two-Phase Critical Flow of One-Component Mixtures in Nozzles, Orifices, and Short Tubes," *J. Heat Transfer, Trans. ASME*, (1971) 179-187.
- [4] L. Bolle, P. Downar-Zapolski, J. Franco, J.M. Seynhaeve, "Experimental and Theoretical Analysis of Flashing Water Flow through a Safety Valve," *J. Hazardous Materials* 46(1996) 105-116.
- [5] Osakabe.M, Isono.M, "Effect of Valve Lift and Disk Surface on Two-Phase Critical Flow at Hot Water Relief Valve," *International Journal of Heat and Mass Transfer*, Vol.39, No.8, (1996) 1617-1624.
- [6] R.E.Henry, R.J.Hammersley,W.E. Berger, B.Deitke, "Two-Phase Critical Flow through Control Valves, *ANS Transaction*, Vol. 79,(1998) pp 340-342.
- [7] D.Abdollahian, A.signh, "Prediction of Critical Flow Rates through Power-Operated Relief Valves," *Second Interna. Topical Meeting on Nuclear Reactor Thermal-Hydraulics*, ANS, Santa Barbara, CA USA, (1982) pp 912-918.
- [8] H.K.Fauske, "The Discharge of Saturated Water Through Tubes," *Chem. Eng. Prog. Symp. Ser.*, Vol.61, (1965) p 210.
- [9] E.B.Wylie and V.L.Streeter, "Fluid Transients," FEB PRESS, (1983) p7.
- [10] D.W.Sallet, " Vapor Flow Rating of Valves Using Small Pressure Reservoirs," *Nuclear Engineering and Design* 72,(1982) 321-327.